Available online at www.sciencedirect.com
ScienceDirect
Journal of Colloid and Interface Science 309 (2007) 176–182
JOURNAL OF Colloid and Interface Science
www.elsevier.com/locate/jcis

Synthesis and stabilization of Prussian blue nanoparticles and application for sensors

Viktória Hornok, Imre Dékány *

Department of Colloid Chemistry, Nanostructured Materials Research Group of the Hungarian Academy of Sciences, University of Szeged, Aradi Vértanúk tere 1, H-6720 Szeged, Hungary

Received 21 December 2006; accepted 5 February 2007

Available online 14 February 2007

Dedicated to professor E. Matijevic on the occasion of his 85th birthday

Abstract

Prussian blue (PB) nanoparticles were synthesized by two methods from $FeCl_2$ and $K_3Fe(CN)_6$ and from $FeCl_3$ and $K_3Fe(CN)_6$ based on the method published by Fiorito et al., and stabilized by different polymers like polyvinyl alcohol (PVA), polyvinyl pyrrolidone (PVP), polyallylamine hydrochloride (PAH), polydiallyl-dimethyldiammonium chloride (PDDA) and polystyrene sulfonate (PSS). The effect of the monomer/Fe^{3+} ratio was studied regarding the average particle size and ζ-potential. The forming PB structure was checked by X-ray diffraction. The stabilization was successful for every applied polymer, but the average particle size significantly differs. Particle size distributions were determined by Malvern type nanosizer equipment and by transmission electron microscope (TEM) and zeta potential values were determined for the obtained stabile samples. The results revealed that by using $FeCl_2$ and $K_3Fe(CN)_6$ for PB preparation particles with narrow size distribution and average diameter of 1.7 nm occurred but stabilization was necessary. By the other method the dispersion was stabile with 182 nm particles but the particle size exponentially decreased to 18 nm with increasing PVP concentration. Ultrathin nanofilms were prepared on glass support by the alternating layer-by-layer (LbL) method from PB particles and PAH. The morphology of the prepared films was investigated also by AFM. The films were immobilized on interdigitated microsensor electrodes (IME) and tested in sensing hydrogen peroxide and different acids like acetic acid, hydrochloric acid vapors.

Keywords: Prussian blue; Nanoparticles; Stabilization by polymers; Sensors

1. Introduction

Prussian blue (PB) as a mixed valance hexacyanomatelate salt is well known to exhibit interesting electro, photochemical, biochemical and magnetic properties [1–4]. These special properties make PB-modified electrodes potentially applicable for sensors [5–7] or electrochromic display devices [8]. Several publications were already concerned with the characterization of these properties in thin films of PB [9–16], which were prepared by different methods from dip-coating to spray technique via Langmuir–Blodgett (LB) deposition [17–22] or SPR technique [23]. Among the different techniques of film preparation, only the LB technique was suitable so far to control the film thickness. The LbL method is reported in this paper, which is based on the multiple sequential adsorption of positively and negatively charged particles on a charged support [24–32]. The method is adapted from the preparation route of inorganic particle films developed by Iler et al. and polyelectrolyte films reported by Decher et al. [33,34]. Structural, thermal [35] and surface thermodynamic properties [36] of the prepared films were studied.

It is well known that PB particles can be prepared by different ways from solutions of Fe^{2+} ions and $[Fe(CN)_6]^{3-}$ ions or from of Fe^{3+} ions and a solution containing $[Fe(CN)_6]^{4-}$ ions or from of Fe^{3+} and $[Fe(CN)_6]^{3-}$ in the presence of H_2O_2. We report on a formation of highly dispersed PB nanoparticles controlled by addition of different polymers, namely polyvinyl pyrrolidone (PVP), polyvinyl alcohol (PVA), and polyallylamine hydrochloride (PAH) solution, polydiallyl-dimethyldiammonium chloride (PDDA) and polystyrene sulfonate (PSS) and by varying the monomer/Fe^{3+} ratio.

* Corresponding author.
E-mail address: i.dekany@chem.u-szeged.hu (I. Dékány).

0021-9797/$ – see front matter
doi:10.1016/j.jcis.2007.02.022

The Prussian blue particles were immobilized onto interdigitated microsensor electrodes (IME) in this study that are widely used in several field of sensor technology based on Langmuir–Blodgett thin films, for studying the environmental effects on polymer thin films. These devices are inert, array microelectrodes formed from patterned nobles metals sputter deposited onto an insulating substrate chip [37–40].

2. Materials and methods

In this paper Prussian blue nanoparticles were synthesized by two methods from $FeCl_3$ and $K_3[Fe(CN)_6]$ in the presence of a slight excess of H_2O_2 based on the method published by Fiorito et al. [41] and by the reaction of $FeCl_2$ and $K_3[Fe(CN)_6]$. The solution of $FeCl_3$ containing a slight excess of H_2O_2 constitute solution I, and similarly $K_3[Fe(CN)_6]$ mixed with the slight excess of H_2O_2 was solution II. Then under continuous stirring, solution I was added to solution II drop wisely to produce solution III. During mixing a blue deposit was observed accompanying with gas bubbles.

The materials used for the experiments were all of analytical grade, the $FeCl_3 \times 6H_2O$ (Reanal), $K_3[Fe(CN)_6]$ (Reanal), $FeCl_2 \times 4H_2O$ (Fluka) and H_2O_2 (Molar) were used to prepare the Prussian blue dispersions. Polymers applied as stabilizing agent were polyvinyl alcohol (Reanal, $M_W = 72{,}000$), polyvinyl pyrrolidone (Fluka, K-40, average $M_W = 40{,}000$), polyallylamine hydrochloride (Aldrich), polydiallyl-dimethyldiammonium chloride (Aldrich, $M_w = 200{,}000$–$30{,}000$) and polystyrene sulfonate (Aldrich, $M_w = 70{,}000$). The solutions used for sensor measurements: hydrochloric acid, acetic acid and hydrogen-peroxide were all Molar products.

Light absorbance of the films was followed by Uvikon 930 UV–vis two-way spectrophotometer. The spectra of the dispersions and the thin film after every dipping cycle were recorded. For representation the $\lambda = 684$ nm data were used and the results were corrected by the absorbance of the medium or the cleaned glass slide. X-ray diffraction measurements (XRD) were performed in a goniometer (Philips PW 1820, CuK_α, 40 kV, 30 mA, Ni grids as filter). Particle size distribution functions and the charges of the colloidal particles were determined by measuring the zeta potential in a Malvern type Nanosizer.

The thermoanalytical measurements were performed by a Mettler Toledo TGA/SDTA851^e type equipment. The morphology of prepared films was characterized by Atomic Force Microscope Nanoscope III type, Digital Instruments, USA, equipped with a scanner with scanning capability of 12.5 μm in x and y direction and 3 μm in z direction. A tapping type tip made of silicon was used (Veeco Nanoprobe Tips RTESP model, 125 μm length, 300 kHz) during measurements. Before preparation the coating of IME electrodes their surface was 5 times washed by propanol and distilled water. The PB dispersions were deposited onto surface of interdigitated microsensor electrodes (IME) for sensor applications and the test reactions were carried out by a Keithly Model 2400 Series SourceMeter. During sensor investigations the current strength through the PB modified IME at a given voltage was detected by computer-control first in air to get a baseline, then the electrode was placed into the closed vapor space while the saturation completed and then take off to air for some minutes and then into the examined next material vapor space or the same but more concentrated vapor. The current signal was detected all along the measurements. The jump in current intensity is characteristic of the concentration of the analyzed sample. The height of current profile means the jump in current strength relative to the current intensity measured in air and in the vapor space of acetic acid for instance. The width of current profile just indicates the time enough for a sensor-target vapor pair to get equilibrium.

3. Results and discussion

It is well known that a blue precipitate of PB is formed, if excess of Fe^{2+} ions are added to a solution containing $[Fe(CN)_6]^{3-}$ ions or excess of Fe^{3+} ions are added to a solution containing $[Fe(CN)_6]^{4-}$ ions or if solutions of Fe^{3+} and $[Fe(CN)_6]^{3-}$ ions are mixed in the presence of H_2O_2 [36]. The chemical reaction of PB formation can be expressed below [42].

$$2Fe^{3+} + 2\big[Fe(CN)_6\big]^{3+} + H_2O_2 + 2K^+ \rightarrow 2KFe\big[Fe(CN)_6\big] + O_2 + 2H^+. \quad (1)$$

3.1. Stabilization of PB dispersion by different polymers

The reference sample synthesized based on Eq. (1) with initial concentration of $[Fe^{2+}]$, $[Fe^{3+}] = 10$ mM, $[H_2O_2] = 5$ mM without added polymer was analyzed by TEM and showed average diameter of 1.7 nm and narrow size distribution but slow sedimentation however (Fig. 1). The PAH, PDDA, PVA, PVP and PSS-stabilized PB nanoparticles were produced by a same way apart from that the polymer solution was mixed to solution $FeCl_3$ before the reduction agent was added to. The stabilization was successful in every type of polymer at identical monomer/$FeCl_3$ ratio = 20:1. The spectra of PB dispersions stabilized by different polymers revealed that the stabilization process takes places different ways according to the

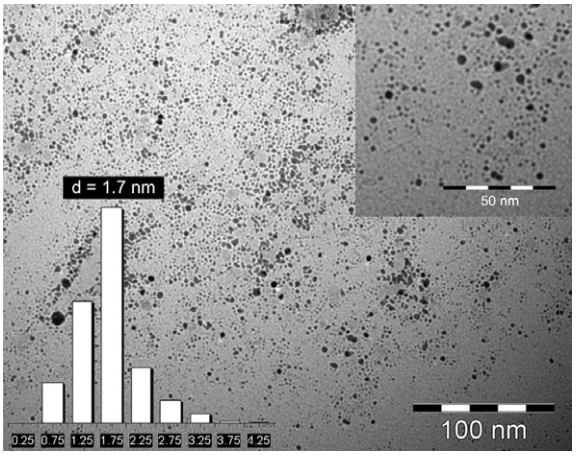

Fig. 1. TEM image of PB prepared from $FeCl_3$ and $K_3Fe(CN)_6$ and H_2O_2 solutions ($[Fe^{2+}]$, $[Fe^{3+}] = 10$ mM, $[H_2O_2] = 5$ mM).

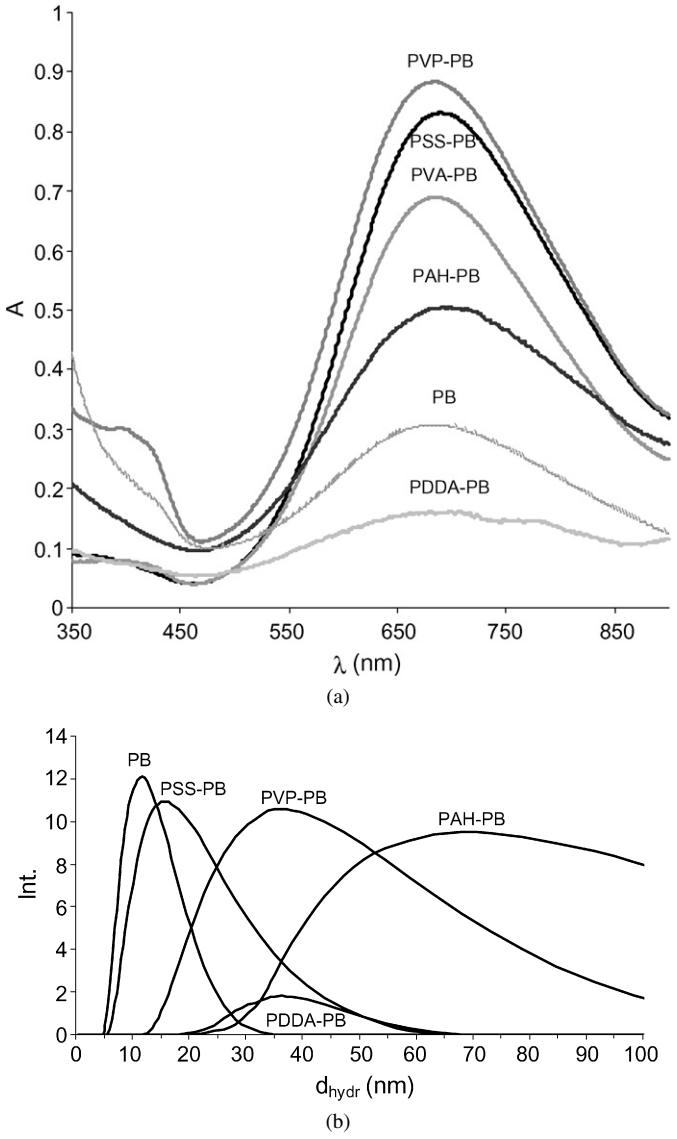

Fig. 2. (a) Spectra of Prussian blue dispersions stabilized by different polymers, at identical monomer/Fe^{3+} ratio = 20:1. (b) Particle size distribution curves of Prussian blue dispersions stabilized by different polymers, at identical monomer/Fe^{3+} ratio = 20:1.

Table 1
Particle size and ζ-potential of PB particles[a] without polymer and stabilized by different polymers

Type of stabilizing polymer	Average particle size (nm)		ζ-Potential nanosizer (mV)
	TEM	Nanosizer	
PB	1.7	11.7	−78
PB-PDDA	33.5	38	−8
PB-PAH	42	70	−22
PB-PSS	4.4	15.7	−61
PB-PVP	38.9	35	−38
PB-PVA	16.1	28	−68

[a] Using H_2O_2 at the preparation process.

charge properties of polyelectrolytes (Fig. 2a). The charge of the prepared PB and polymer stabilized PB dispersions was characterized by Malvern Nanosizer instrument (Table 1). The

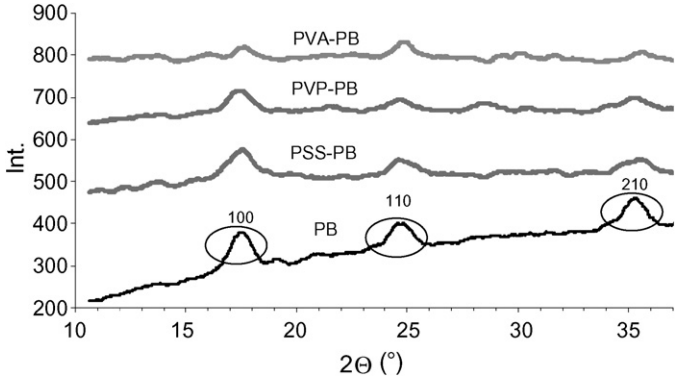

Fig. 3. XRD patterns of PB without polymer and PB stabilized by different polymers, at identical monomer/Fe^{3+} ratio = 20:1.

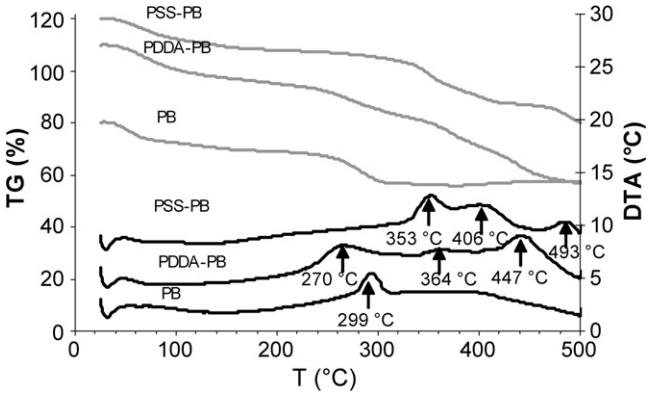

Fig. 4. Thermoanalytical measurements of polymer protected PB (monomer/Fe^{3+} ratio = 20:1).

average particle diameters of the formed PB dispersions were also determined by the Nanosizer and were examined in electron microscope the particle size distribution show monodisperse particles (Fig. 2b). The results obtained by electron microscope and Malvern nanosizer show good agreement (Table 1). In case of positively charged polymers the nanoparticle aggregation occurs through electrostatic attraction between the negatively charged particles and the polymer chain carrying positive charges (PDDA-PB), because of the ζ-potential is only −8 mV. In the case of the negatively charged or uncharged polymers surrounds the particles and the identical charges retard aggregation and in addition increases stability ($\zeta = -38$–68 mV).

The X-ray powder diffraction (XRD) pattern of the powder at any applied polymer showed peaks at 17.6° (100), 24.8° (110), 35.2° (200), 39.6° (210) and 43.5° (Fig. 3) characteristic of Prussian blue crystalline structure [42,43].

Thermoanalytic measurements were used to control the thermostability of PB and polymer protected PB powder (Fig. 4). The presence of polymer do not influences the first endothermic mass loss of water (40 °C) but shifts the exothermic second one corresponds (299 °C) to lower temperatures in case of PDDA (270 °C), but to higher temperatures in case of PSS (353 °C).

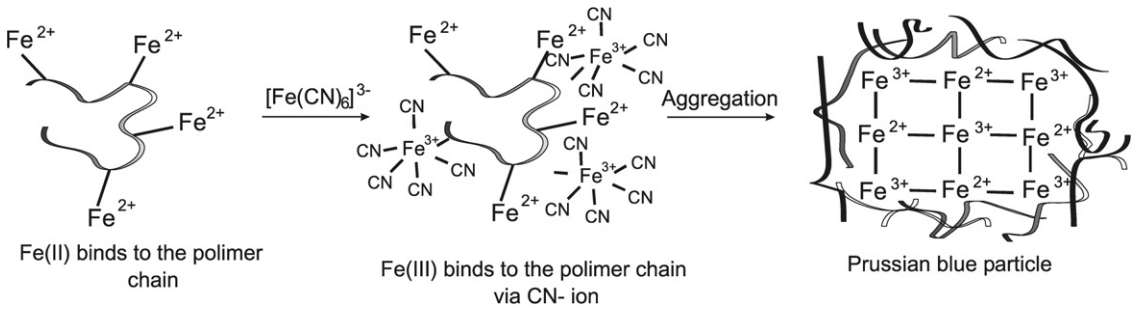

Fig. 5. Stabilization mechanism of PB by polymers.

Table 2
Particle size and ζ-potential of PB particles[a] without polymer and stabilized by PVP at different monomer/Fe^{3+} ratio

PVP monomer/ Fe^{2+} ratio	Average particle size (nm)		ζ-Potential nanosizer (mV)
	TEM	Nanosizer	
Without PVP	184	220	−20.9
2:1	84	122	−23.9
5:1	51	58.8	−24
10:1	42	43.5	−24.8
20:1	31	37.8	−21.4
40:1	23	32.7	−15.3
100:1	18	21	−10.4

[a] Without using H_2O_2 at the preparation process.

3.2. Stabilization of PB dispersion by PVP at different monomer Fe^{3+} ratio

In the case of neutral PVP the monomer-Fe^{3+} ratio was changed from the polymer free dispersion to 100:1 PVP monomer to Fe^{3+} ratio. During preparation equimolar amounts of aqueous $FeCl_2$ and $K_3[Fe(CN)_6]$ solutions were mixed in the presence of PVP with final concentrations of $[Fe^{2+}]$, $[Fe^{3+}] = 10$ mM, readily producing an intensive blue color. Formation of the PVP-protected PB nanoparticles is schematized (Fig. 5). The Fe^{2+} ions bind to the polymer chain and during $K_3[Fe(CN)_6]$ addition and aggregation process forms a mixed valance blue-colored complex [43].

The size of PB particles formed from solution of $K_3[Fe(CN)_6]$ and $FeCl_2$ was 182 nm determined by TEM and nanosizer (Table 2). The UV–vis spectrum of the resulting solution showed a broad absorption with λ_{max} at 684 nm (Fig. 6), which is consistent with an intermetal charge-transfer band from Fe^{2+} to Fe^{3+} in PB [44,45].

Effect of polymer amount was studied in case of PVP. The average particle size function follows exponential character from 184 nm to 18 nm if the monomer/Fe^{3+} ratio decreased from the polymer free dispersion through 2:1 to 100:1 at given Fe^{2+}, Fe^{3+} concentrations (Figs. 7a and 7b).

3.3. Preparation of PB/polymer thin films on glass surface

In order to characterize the PB films prior to film preparation on electrodes, the dispersions were deposited onto glass support. The process was controlled by spectroscopic measurements. The absorbance measurements verify the successful film formation, the absorbance increases with increasing cycle number.

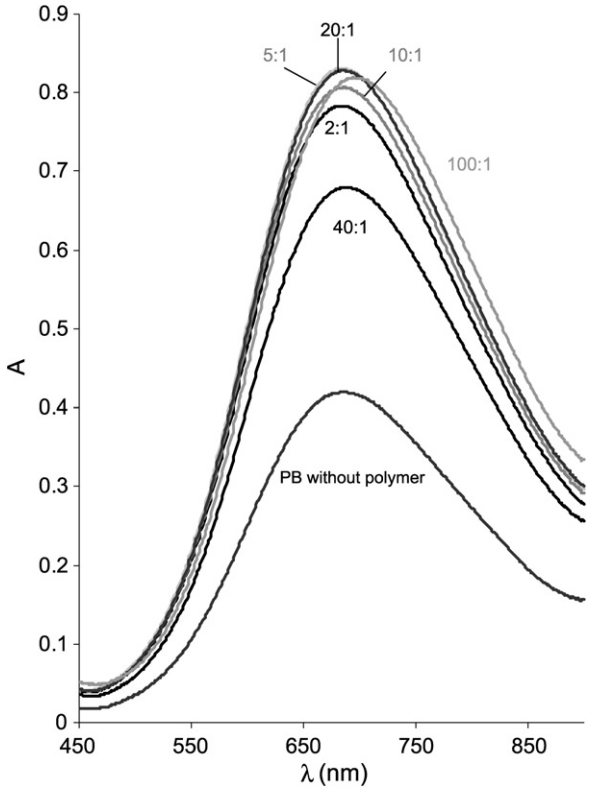

Fig. 6. Spectra of Prussian blue dispersions stabilized by PVP, at various monomer/Fe^{3+} ratio.

The nanofilms were prepared on glass surfaces by the layer-by-layer immersion technique. Previous to film preparation the glass slides were cleaned in chromic acid for hours to remove all the contamination, washed with distilled water and dried. The glass surface is negatively charged and forms thin films if we immerse into positively charged polymer solution for 10 min to form a polymer layer. This procedure must be followed by rinsing with distilled water in order to remove the weakly adsorbed macromolecules. The positively charged PAH (0.01 w/v%, 0.25, 0.5 and 0.1 w/v%) polymer chain film then binds negatively charged PB particles when immersed into the PB dispersion (Fig. 8). The immersion period took 10 min followed by half a minute rinsing with distilled water and drying with N_2. Light absorbance of each bilayer was recorded and shows linear increase with the number of PAH (0.01 w/v%)/PB layers (Fig. 9). Morphology of the prepared films was controlled by AFM. The PAH (0.01 w/v%)/PB films of 5 cycles

quite homogeneous the characteristic spherical PB particles with 3.6 nm roughness value according to the image (Fig. 10). The 54 nm diameter of nearly monodisperse particles is the size of adhered PB particles and polymer cover.

3.4. Sensor measurements on intredigitated microsensor electrodes

Application of PB is widespread due to the different oxidal state of iron in the compound. During our experiments sandwiched-like (LbL) structure was produced on the surface of interdigitated microelectrodes or 0.5 ml drop of the dispersion was dried onto the electrode to gain thicker layer and the current strength was recorded at a given voltage. For the measurements the PB dispersion prepared from Fe^{3+}, $[Fe(CN)_6]^{3-}$ and H_2O_2 solutions was used. The detected target molecule concentration denoted in w/v% concerned to the liquid-phase amount.

The Prussian blue-modified electrodes conductive through their hydrate shell so they work only in the presence of water. Accordingly, high current response was obtained in case of water vapor sensing. PB is known to be a superior electrocatalyst in hydrogen peroxide reduction and monitoring of levels of H_2O_2 is of great importance for modern medicine, environmental control, and various branches of industry [46]. Our electrodes proved to be effective electrodes in H_2O_2 sensing.

The PB-based sensors were tested in sensing different compounds like water, H_2O_2 and acid vapors (Fig. 11). The highest current was detected in case of acetic acid by using a dropped dried PAH-PB film. The current intensity is increasing between 50–75 s, because this is the reaction time of the sensing effect. During our experiments, several polymers were checked as film forming agent with PB in the sensing of hydrochloric acid, acetic acid, and sulfuric acid, PAH proved to be the best polymer to immobilize the particles on the IME surface both regarding the highest sensitivity and the currant signal intensity. The PB nanoparticles of 1.7 nm, possess high sensitivity in detection of acetic acid according to our measurements. If we use PAH (0.1 w/v%)/PB film sensor at 0.2 V (at 0.5 mg

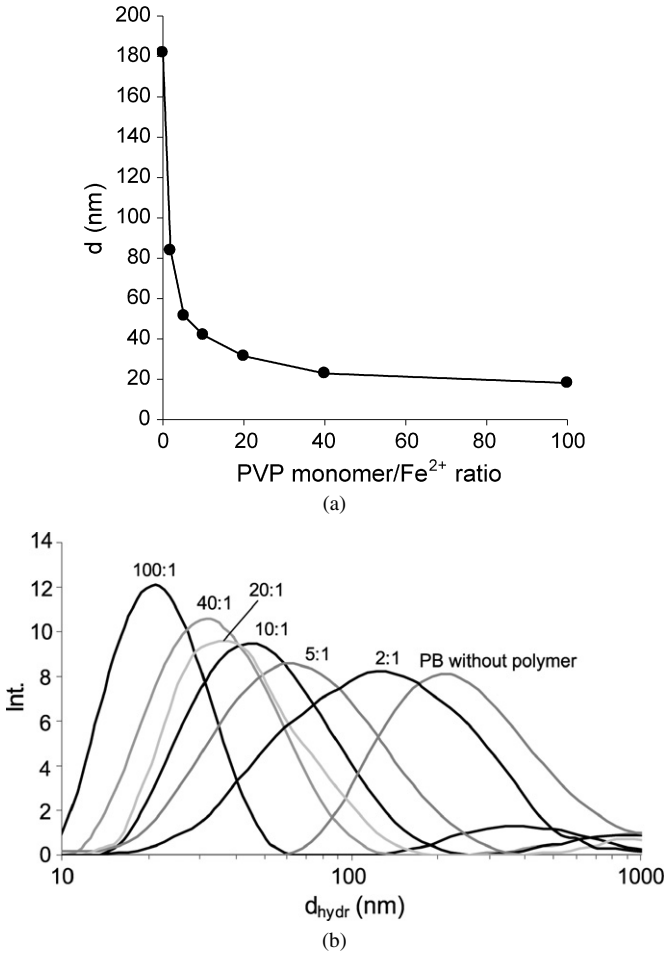

Fig. 7. (a) The influence of monomer:Fe^{3+} ratio on the average particle size of PB particles. (b) Particle size distribution curves of Prussian blue dispersions stabilized by PVP, at different monomer/Fe^{3+} ratio.

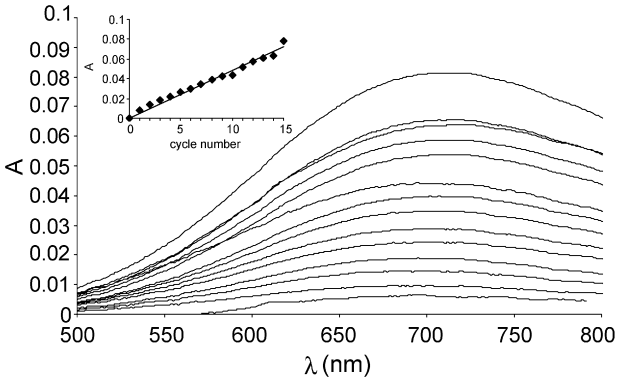

Fig. 9. Absorbance of PAH/PB films with increasing layer number (λ = 684 nm).

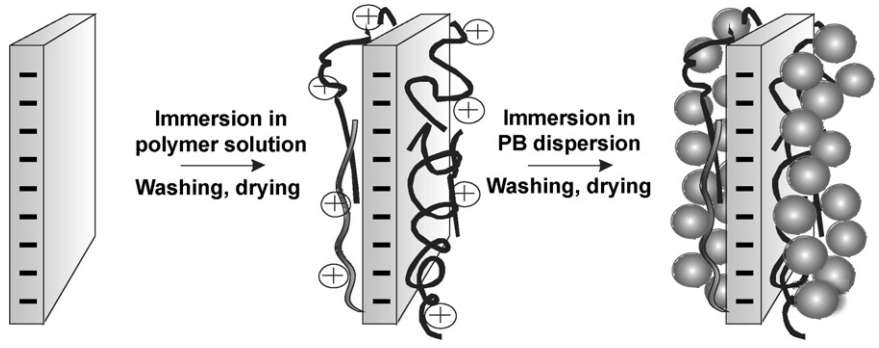

Fig. 8. Schematic illustration of film preparation from PB dispersions and polymers by the LbL immersion technique.

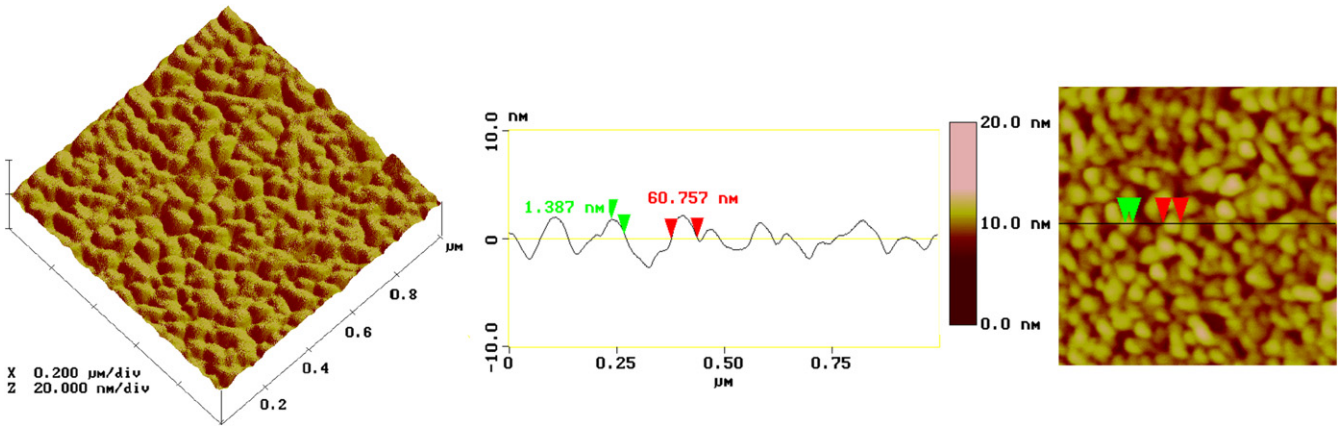

Fig. 10. AFM image of nearly monodisperse Prussian blue deposited by PAH ($n = 5$, 1 µm × 1 µm).

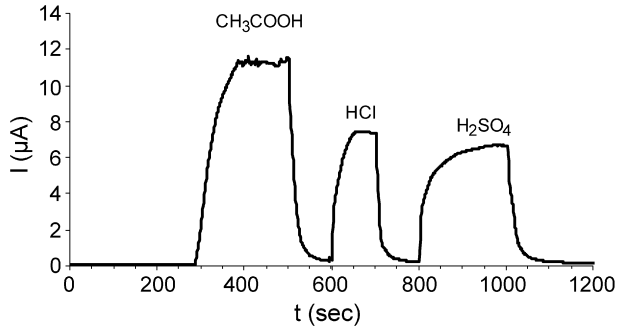

Fig. 11. Current signal of PAH (0.1 w/v%)/PB film ($n = 1$) on IME for different acid vapors (0.2 V, 0.5 mg/cm^2).

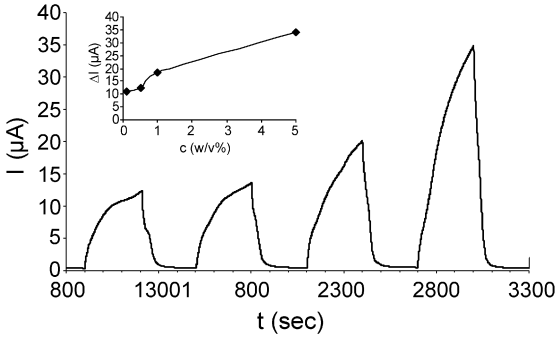

Fig. 12. Current signal of PAH (0.1 w/v%)/PB film ($n = 1$) on IME for acetic acid vapor at different concentrations (0.2 V, 0.5 mg/cm^2).

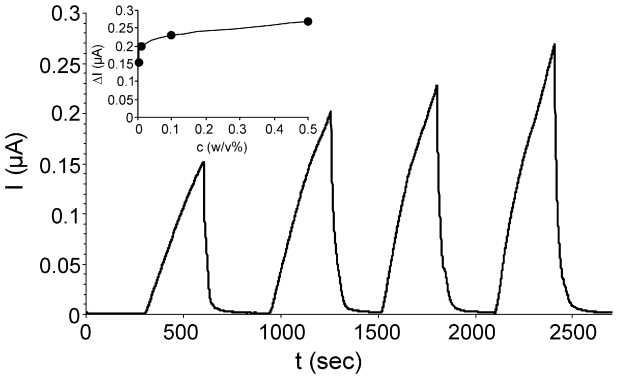

Fig. 13. Current signal of PAH (0.01 w/v%)/PB film ($n = 5$, LbL) on IME for hydrochloric acid vapor at different concentrations (2 V).

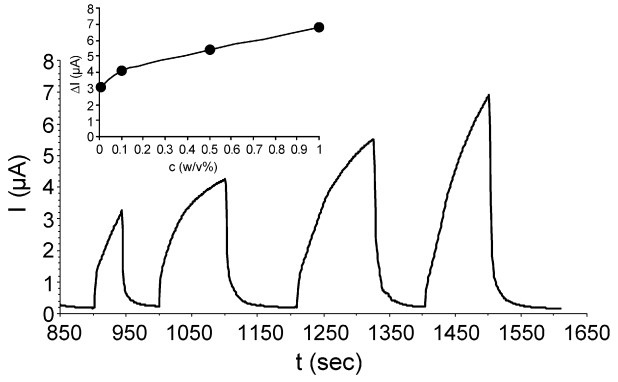

Fig. 14. Current signal of PAH (0.1 w/v%)/PB film ($n = 1$) on IME for hydrogen peroxide vapor at different concentrations (0.2 V, 0.5 mg/cm^2).

PB/cm^2 coating) the jump in current intensity is $\Delta I = 12$ µA with increasing concentration (0–0.01 w/v%) supposed to the preferential adsorption of acetic acid in the vapor phase on the surface of the PB nanoparticles (Fig. 12). Similarly, the 5 cycles of alternately deposited (LbL) PB and PAH (0.01%) film sensor detect lower current at higher voltage (2 V) due to the less amount of PB in the surface in hydrochloric acid sensation although saturation behavior occurs in current with increasing concentration (Fig. 13).

Our PAH/PB sensors were tested in the detection of hydrogen peroxide. Hydrogen peroxide concentration series (0.01, 0.1, 0.5 and 1 w/v% in water) were prepared. The concentration of the film constituting polymer was 0.1 w/v%. The concentration dependence shows saturation profile, the certain ΔI values concern to the different peroxide amounts are represented in Fig. 14.

4. Summary

Prussian blue and polymer protected PB dispersions with arbitrary particle diameter from 1.7 up to 184 nm were successfully prepared from $K_3[Fe(CN)_6]$ and $FeCl_3$ by using H_2O_2 solution or from $K_3[Fe(CN)_6]$ and $FeCl_2$ solutions. The size of PB particles can be tuned by the preparation method, the type and amount of polymer and iron ion ratio. Well-ordered ultra-

thin PAH/PB nanofilms were prepared on glass and interdigitated microelectrodes support and the film thickness increased linearly with dipping cycles. The results show that PAH/PB films were the most appropriate for sensor application due to the highest current response. The films were successfully tested in sensing hydrogen peroxide and different acids like acetic acid and hydrochloric acid. The sensor sign intensity reagent concentration functions show saturation characteristic.

Acknowledgment

The authors wish their thanks for the financial support of the Péter Pázmány program of the Hungarian National Office of Research and Technology (No. RET-07/2005).

References

[1] K. Itaya, I. Uchida, V.D. Neff, Acc. Chem. Res. 19 (1986) 162.
[2] R.J. Mortimer, Chem. Soc. Rev. 26 (1993) 147.
[3] M. Kaneko, J. Macromol. Sci. Chem. A 24 (1987) 357.
[4] S. Ferlay, T. Mallah, R. Ouahès, P. Veillet, M. Verdaguer, Nature 378 (1995) 701.
[5] I. Del Villar, I.R. Matias, F.J. Arregui, J. Echeverría, R.O. Claus, Sens. Actuators B 108 (2005) 751.
[6] R. Koncki, O.S. Wolfbeis, Sens. Actuators B 51 (1998) 355.
[7] M.P. O'Halloran, M. Pravda, G.G. Guilbault, Talanta 55 (2001) 605.
[8] S. Ravaine, C. Lafuente, C. Mingotaud, Langmuir 14 (1998) 6347.
[9] V.D. Neff, J. Electrochem. Soc. 125 (1978) 886.
[10] N. Toshima, K. Liu, M. Kaneko, Chem. Lett. 19 (1990) 485.
[11] K. Itaya, T. Ataka, S. Toshima, J. Am. Chem. Soc. 104 (1982) 4767.
[12] A.L. Crumbliss, P.S. Lugg, N. Morosoff, Inorg. Chem. 23 (1984) 4701.
[13] A. Dostal, B. Meyer, F. Scholz, U. Schröder, A.M. Bond, F. Marken, S.J. Shaw, J. Phys. 99 (1995) 2096.
[14] N. Kimizuka, T. Asai, S. Ohno, K. Fujiyoshi, T. Kunitake, Surf. Sci. 386 (1997) 245.
[15] Y. Guo, A.R. Guadalupe, O. Resto, L.F. Fonseca, S.Z. Weisz, Chem. Mater. 11 (1999) 135.
[16] K. Honda, J. Ochiai, H. Hayasi, J. Chem. Soc. Chem. Commun. (1986) 168.
[17] K. Ariga, Y. Lvov, I. Ichinose, T. Kunitake, Appl. Clay Sci. 15 (1999) 137.
[18] M. Onda, K. Ariga, T. Kunitake, J. Biosci. Bioeng. 87 (1999) 69.
[19] Y. Lvov, K. Ariga, M. Onda, I. Ichinose, T. Kunitake, Colloids Surf. A 146 (1999) 337.
[20] T. Kunitake, Thin Solid Films 9–12 (1996) 284.
[21] Y. Lvov, S. Yamada, T. Kunitake, Thin Solid Films 300 (1997) 107.
[22] M. Szekeres, O. Kamalin, R.A. Schoonheydt, K. Wostyn, K. Clays, A. Persoons, I. Dékány, J. Mater. Chem. 11 (2002) 3268.
[23] M. Szekeres, A. Széchenyi, K. Stepan, T. Haraszti, I. Dékány, Colloid Polym. Sci. 283 (2005) 937.
[24] M. Szekeres, O. Kamalin, P.G. Grobet, R.A. Schoonheydt, K. Wostyn, K. Clays, A. Persoons, I. Dekany, Colloids Surf. A 1–3 (2003) 77.
[25] I.L. Radtchenko, G.B. Sukhorukov, S. Leporatti, G.B. Khomutov, E. Donath, H. Möhwald, J. Colloid Interface Sci. 230 (2000) 272.
[26] G.B. Sukhorukov, H. Möhwald, G. Decher, Y.M. Lvov, Thin Solid Films 284–285 (1996) 220.
[27] I. Dékány, T. Haraszti, Colloids Surf. A 123–124 (1997) 391.
[28] N.A. Kotov, T. Haraszti, L. Túri, G. Zavala, R.E. Geer, I. Dékány, J.H. Fendler, J. Am. Chem. Soc. 119 (1997) 6821.
[29] R. Steitz, V. Leiner, R. Siebrecht, R. von Klitzing, Colloids and Surfaces A 163 (2000) 63.
[30] R. von Klitzing, H. Möhwald, Macromolecules 29 (1996) 6901.
[31] J.E. Wong, F. Rehfeldt, P. Haenni, M. Tanaka, R. von Klitzing, Macromolecules 37 (2004) 7285.
[32] R. von Klitzing, B. Tieke, Adv. Polym. Sci. 165 (2004) 177.
[33] R.K. Iler, J. Colloid Interface Sci. 21 (1966) 569.
[34] G. Decher, J.D. Hong, Thin Solid Films (1992) 210.
[35] Y. Lvov, G. Decher, H. Möhwald, Langmuir 9 (1993) 481.
[36] S. Köstler, A.D. Delgado, V. Ribitsch, J. Colloid Interface Sci. 286 (2005) 339.
[37] A. Guiseppi-Elie, A.M. Wilson, J.M. Tour, T.W. Brockmann, P. Zhang, D.L. Allara, Langmuir 11 (1995) 1768.
[38] S.R. Mikkelsen, G.A. Rechnitz, J.M. Tour, T.W. Brockmann, P. Zhang, D.L. Allara, Anal. Chem. 61 (1989) 1737.
[39] S.T. Kowel, G.-G. Zhou, M.P. Srinivasan, P. Stroeve, B.G. Higgins, Thin Solid Films 134 (1985) 209.
[40] H.B. Dietmar, A. Guiseppi-Elie, Curr. Opin. Biotechnol. 12 (2001) 41.
[41] P.A. Fiorito, V.R. Gonçales, E.A. Ponzio, S.I. Córdoba de Torresi, Chem. Commun. (2005) 366.
[42] M. Pyrasch, B. Tieke, Langmuir 17 (2001) 7706.
[43] T. Uemura, S. Kitagawa, J. Am. Chem. Soc. 125 (2003) 7814.
[44] S.-Q. Liu, J.-J. Xu, H.-Y. Chen, Electrochem. Commun. 4 (2002) 421.
[45] M. Pyrasch, B. Tieke, Adv. Mater. 13 (2001) 1188.
[46] A.A. Karyakin, E.A. Purganova, I.A. Budashov, I.N. Kurochkin, E.E. Karyakina, V.A. Levchenko, V.N. Matveyenko, S.D. Varfolomeyev, Anal. Chem. 76 (2004) 474.